
The Mechanisms of Creep in Olivine [and Discussion]

C. Goetze and J. P. Poirier

Phil. Trans. R. Soc. Lond. A 1978 **288**, 99-119

doi: 10.1098/rsta.1978.0008

Email alerting service

Receive free email alerts when new articles cite this article - sign up in the box at the top right-hand corner of the article or click [here](#)

To subscribe to *Phil. Trans. R. Soc. Lond. A* go to: <http://rsta.royalsocietypublishing.org/subscriptions>

The mechanisms of creep in olivine

BY C. GOETZE

Department of Earth and Planetary Sciences, Massachusetts Institute of Technology, Cambridge, Massachusetts 02139, U.S.A.

We summarize the progress made in providing experimental verification for the deformation map of polycrystalline olivine published by Stocker & Ashby in 1973 (*Rev. Geophys.* **11**, 391). Porosity-free polycrystalline deformation data, applicable to the mantle, were found to be obtainable only from high-pressure deformation studies. Combination of the results of such studies with hardness measurements and single crystal deformation studies on olivine provides narrow constraints on the flow of olivine resulting from dislocation mechanisms from room temperature to the melting point along a band of experimentally accessible strain rates. A good fit is obtained combining a Dorn law above 2 kbar differential stress,

$$\dot{\epsilon}/s^{-1} = 5.7 \times 10^{11} \exp \left\{ -\frac{128 \text{ kcal/mol}}{RT} \left(1 - \frac{\sigma_1 - \sigma_3}{85\,000} \right)^2 \right\},$$

with a power law below 2 kbar,

$$\dot{\epsilon} = 70(\sigma_1 - \sigma_3) \exp \{ -122(\text{kcal/mol})/RT \},$$

where stress is measured in bars (1 bar = 10^5 Pa). Indirect data on a mechanism phenomenologically resembling the Coble creep régime are now available from two sources. The observed strain rates are only slightly faster than those predicted by Stocker & Ashby (1973). The ‘wet’ data, previously believed to show hydrolytic weakening, are found to fall within this Coble field. The asthenosphere is still expected to deform by the dislocation mechanism summarized by the two formulae given above, but higher stress deformation within the lithosphere is almost certainly dominated by this Coble creep régime once dynamic recrystallization sets in.

INTRODUCTION

The creep properties of dunite have been the subject of a considerable literature in the geological sciences since the general acceptance of the theory of plate tectonics. Those not familiar with the setting of this creep problem are referred to figure 1, where the principal terms are defined and orders of magnitude of relevant parameters given.

Localized deformation occurs within the lithosphere; however, this region is generally accepted to move as a number of discrete ‘plates’ over the surface of the Earth at velocities of a few centimetres per year. The corresponding convective motions are continuous and widespread in the asthenosphere to unknown depths. The orthorhombic mineral olivine of the approximate composition $(\text{Mg}_{0.91}\text{Fe}_{0.09})\text{SiO}_4$ is the dominant phase only to about 375 km depth, below which the spinel phase of the same composition, of unknown creep properties, dominates the creep process. Clearly, a study of the creep of olivine, even if complete, leaves the mechanical properties of the deeper mantle unknown. Nevertheless, a large number of more local problems involving the formation of new plates, the collision of plates, the decoupling of plates from the asthenosphere, and the response of plates to vertical loads, to name a few, can be effectively studied without such knowledge.

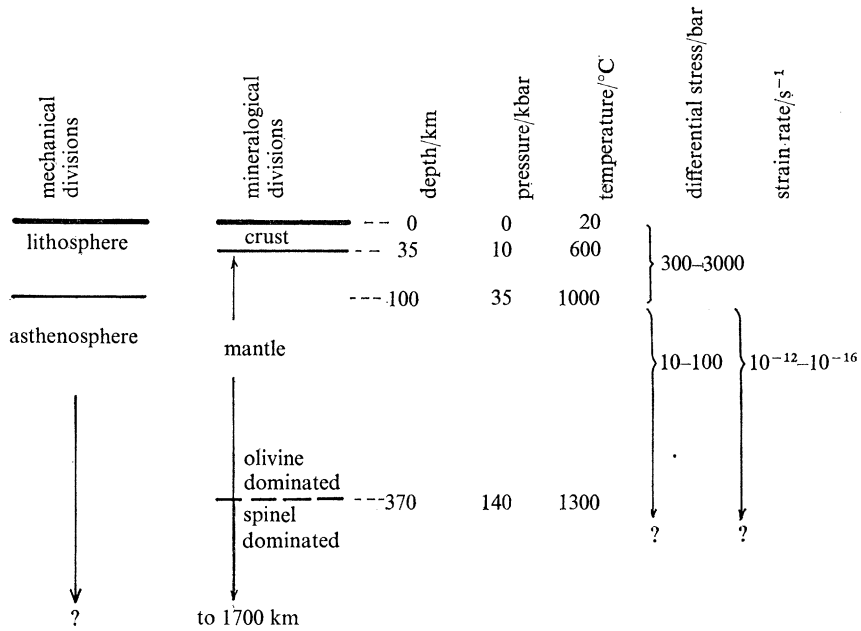


FIGURE 1. Sketch of the principal subdivisions of the Earth in the first 400 km.

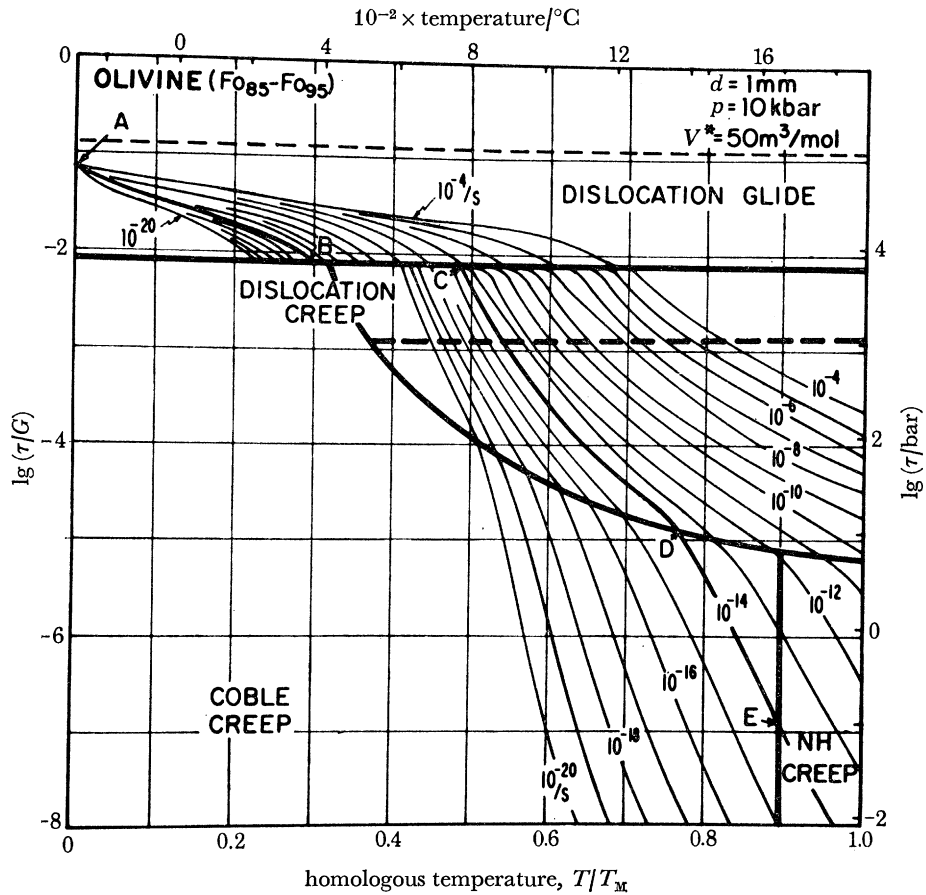


FIGURE 2. Deformation map of olivine predicting the strength developed at each temperature as a function of strain rate. Reprinted from Stocker & Ashby (1973).

Even this upper portion of the mantle is not composed exclusively of olivine but contains 20–50 % pyroxenes, aluminous spinel, garnets, etc. Work has been done on the creep properties of some pyroxene and spinel compositions; however, the creep strengths are similar to those of olivine, and because of their smaller volumetric abundance they are expected to affect the creep properties of the mantle only to a minor extent. The approximation is therefore made that creep of the mantle in the depth range 35–375 km is the creep of olivine.

TABLE 1. APPROXIMATE COMPOSITION, BY MASS,
OF MANTLE-DERIVED OLIVINE

	alpine	xenolith
SiO ₂	40.96	40.30
TiO ₂	0.01	0.15
Al ₂ O ₃	0.21	0.25
Fe ₂ O ₃	0.00	0.00
FeO	7.86	10.26
MnO	0.13	0.09
MgO	50.45	48.60
CaO	0.15	0.07
Na ₂ O	0.01	0.04
K ₂ O	0.00	0.03
H ₂ O ⁺	0.29	0.33
	100.35	100.56

The alpine sample, from Dun Mountain, New Zealand, is believed to have reached the Earth's surface from the mantle by tectonic processes. The xenolith sample is obtained from nuggets entrained by a basalt flow originating within the mantle below Ichinomegata, Japan. Data are from Deer, Howie & Zussman (1964).

In 1973 Stocker & Ashby presented a 'deformation map' predicting the flow of polycrystalline olivine as a function of temperature, strain rate, and differential stress. It is reproduced in figure 2. A small number of data were then available near the boundary of the fields labelled 'dislocation glide' and 'dislocation creep'. The remainder of the map was based on systematics (rules of thumb obtained from a broad range of materials). We summarize here the progress made in a number of laboratories around the world to provide experimental verification for this plot. Let me say in advance that, on the whole, only comparatively minor changes have resulted from this work.

The tools employed have included solid medium high pressure deformation apparatus used to 1300 °C, and 15 kbar (Post 1973; Carter & Ave' Lallemand 1970; Raleigh & Kirby 1970; Blacic 1972) gas medium high pressure apparatus used to 1000 °C and 6 kbar (Goetze & Brace 1972), a 1 atm single crystal deformation apparatus used to 1700 °C (Kohlstedt & Goetze 1974; Durham & Goetze 1977*a, b*), hot hardness apparatus used to 1500 °C (Evans & Goetze 1977), as well as, of course, optical and electron microscopes for the analysis of both experimentally and naturally deformed specimens. Starting materials have been natural rocks of almost pure olivine composition (dunite) and single crystals of gem quality olivine from Arizona and Egypt. Only recently have artificially grown single crystals of adequate size been available, and these only of the magnesian end member. A comparison creep study showed that these differed only to a very minor extent from the natural material, differences which could be ascribed to their difference in iron content (Durham & Goetze 1977*b*). The purity of a typical olivine crystal derived from the mantle can be judged from the compositions given in table 1.

EFFECT OF PRESSURE

The principal purpose for studying the deformation of olivine and olivine-rich aggregates has been to obtain data relevant to the interpretation of motions occurring within the mantle at pressures ranging from 20–130 kbar. Since practically all experiments have been conducted at lower pressures than this, there is a need to extrapolate the results into this range.

It is a common observation that brittle materials such as rocks show a strong pressure sensitivity when deformed in a range of pressure, temperature, stress and strain rate for which some fracturing or cataclasis occurs (Handin 1966). At high temperatures, many ceramic materials are also known to deform through processes in which porosity develops as the specimen strains (Langdon, Cropper & Pask 1971). The development of even a slight porosity introduces a strong pressure sensitivity to the strength which eliminates such mechanism from consideration in the Earth's mantle. Rocks are particularly susceptible to weakening by porosity-forming creep mechanisms, as the primary slip systems of most rock-forming minerals are completely inadequate to meet the Von Mises condition for uniform strain and the formation of porosity permits a considerable relaxation of the Von Mises constraints. This has been shown to be true for MgO, talc, pyrophyllite, graphite, and BN (Paterson & Weaver 1970; Edmond & Paterson 1971; Paterson & Edmond 1972; Edmond & Paterson 1972; Auten & Radcliffe 1976). Early work on rocks at room pressure (Eaton 1968; Murrell & Chakravarty 1973; Misra & Murrell 1965) have all been shown to be porosity-weakened when compared with later high pressure results (Goetze 1971; Goetze & Brace 1972). Unpublished low-pressure creep data on hot-pressed olivine samples of high quality in our laboratory at the lowest practical stresses near the melting point showed clear porosity-weakening. This was evident under the microscope and by comparison with high pressure creep data. The conclusion is therefore that for aggregates of rock-forming minerals, the application of pressures exceeding the differential stresses is required to achieve purely plastic deformation (Edmond & Paterson 1972).

Confining our attention henceforth to pore-free creep experiments, there remains the more modest but not negligible effect of pressure on glide, climb, and the relevant diffusivities. Although creep data have been reported to 30 kbar, they have not so far been of sufficient accuracy to permit any direct observation of these pressure effects. There are at present no less than four groups working on this problem. Under the assumptions that climb limits the creep rate, that oxygen diffusivity limits the climb rate, and that the activation volume for oxygen diffusivity is given by the crystallographically determined volume of the oxygen site in the undisturbed olivine lattice, one predicts a pressure effect on the creep rate of about four orders of magnitude in strain rate at the olivine/spinel boundary (Weertman 1970; Goetze & Brace 1972). The uncertainty in this estimate is believed to be about a factor of 3 in either direction, and seriously limits the usefulness of low pressure creep data below the first 100 km.

As the experimental data are almost exclusively obtained at or below 15 kbar pressure, we restrict the remainder of this discussion to porosity-free but 'low pressure' data. The curves so obtained (figures 3, 4, 6, 10–12) are believed to be applicable to the first 100 km into the Earth without serious correction.

The range of variables of greatest geological interest include strain rates near 10^{-16} to 10^{-12} s⁻¹ and stresses in the deep mantle of 10–100 bar and in the upper mantle of up to a few kilobars. As these conditions were predicted by Stocker & Ashby (figure 2) to fall in the 'dislocation creep' field, and because of the greater experimental accessibility of this field, the majority of the data

in hand occur within this field along a band of experimentally accessible strain rates in the range 10^{-8} to 10^{-3} s^{-1} .

A comparison of Stocker & Ashby's (1973) predictions with currently available polycrystalline data is shown in figure 3, where Stocker & Ashby's predictions show as dotted lines. The data sources are indicated in the figure caption. We plot here a subset of the original data points, falling within the range of strain rates from 10^{-6} to 10^{-4} s^{-1} , corrected to a common strain rate of 10^{-5} s^{-1} according to the formula:

$$\frac{1}{T_{\text{corr}}} - \frac{1}{T_{\text{actual}}} = \frac{R \ln(\dot{\epsilon}_{\text{ac}}/10^{-5})}{125 \text{ kcal/mol}} \quad (1)$$

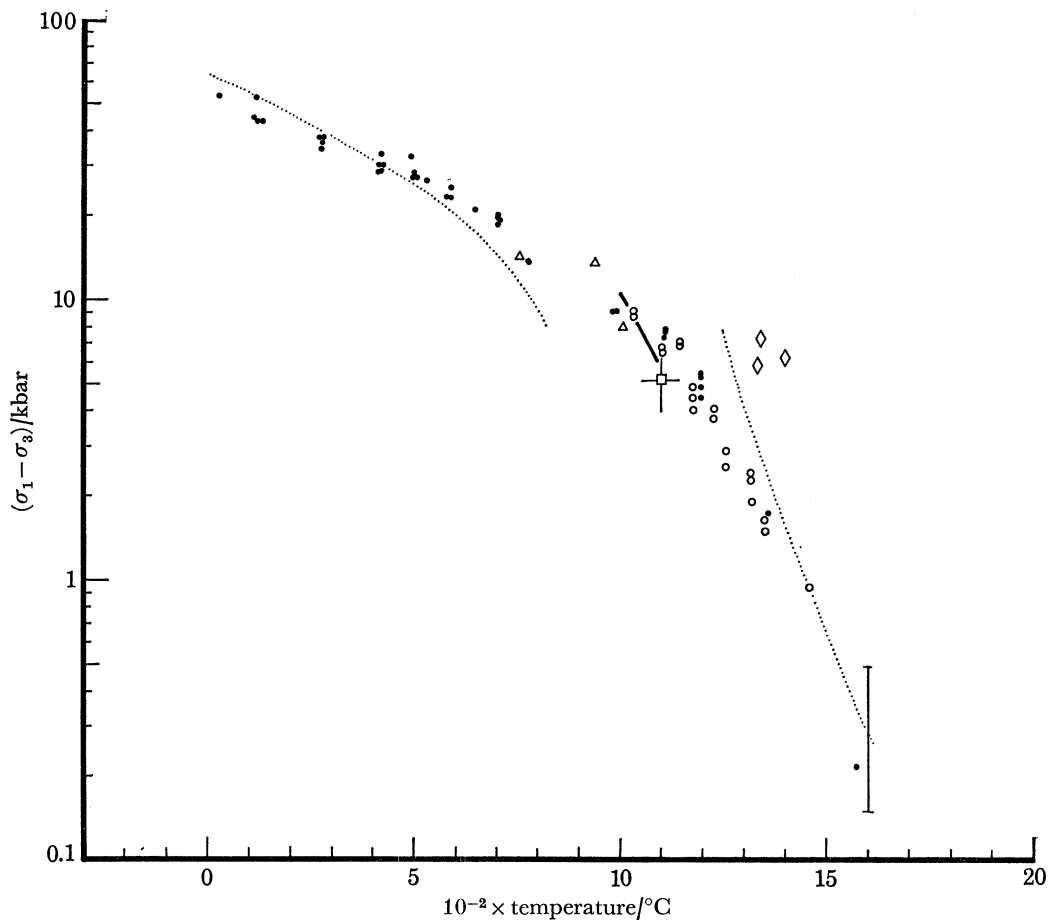


FIGURE 3. A comparison of the experimental creep data on 'dry' polycrystalline olivine aggregates (○, Carter & Ave' Lallemand 1970; solid line, Raleigh & Kirby 1970; △, Blacic 1972; □, Kirby & Raleigh 1973; ◇, Post 1973). Hardness (●, Evans & Goetze 1977) and single crystal bounds (lower right, Durham & Goetze 1977) with Stocker & Ashby's predictions (1973) which are shown as dotted lines. All data have been corrected to a common strain rate of 10^{-5} s^{-1} (see text).

where 'actual' refers to the values measured and 'corrected' indicates the corresponding temperature plotted in figure 3. R is the gas constant. As the corrections for one decade in strain rate are comparatively minor and the apparent activation energy (125 kcal/mol) is well established (see figure 10), we regard this step as uncontroversial. A similar comparison would be obtained for other strain rates falling in the experimental range. What is controversial is that we have excluded a second set of data, labelled by most authors as 'wet', which is obtained in a

solid medium apparatus, with talc as the pressure medium, under conditions in which the talc breaks down and gives off water. This second set of data differs significantly from the first and will be discussed below under *grain-size sensitive creep* (Blacic 1972; Carter & Ave' Lallemand 1970; Post 1973).

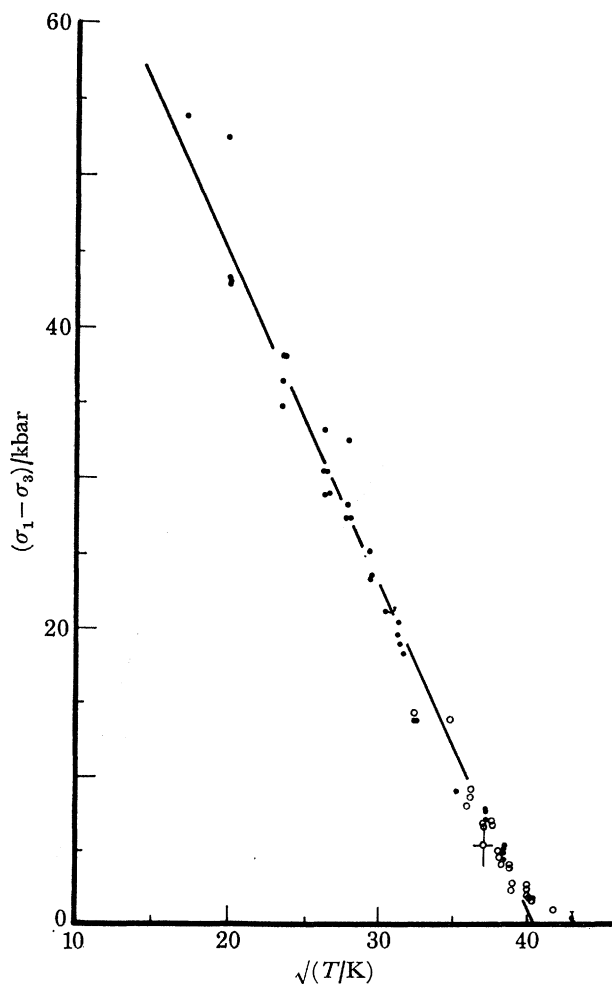


FIGURE 4. The data from figure 3 replotted as $\sigma_1 - \sigma_3$ against \sqrt{T} . A straight line on this plot indicates a perfect fit to equation (2). Parameters for the line shown are $\sigma_p = 85 - 2.094T^{\frac{1}{2}}$. By measurements of the rate sensitivity at 530 °C, the value of Q was set at 128 ± 5 kcal/mol, giving the parameters

$$\begin{aligned}\dot{\epsilon}_0 &= 5.7 \times 10^{11} \text{ s}^{-1}, \\ Q &= 128 \text{ kcal/mol}, \\ \sigma_p &= 85 \text{ kbar}.\end{aligned}$$

A few comments should be made about figure 3.

(a) Work-hardening becomes pronounced above *ca.* 10 kbar stress. In this range a nominal strain of 8% has been used in figure 3 for comparison with the hardness data which are shown as solid circles. At lower stresses a steady-state condition is achieved in less than 5% strain.

(b) Details of the analysis of the hardness data are contained in Evans & Goetze (1977). Hardness data have been corrected to uniaxial yield according to the reduction factors given by Johnson (1970). High-pressure (pore-free) yield data, where available, are in very good agreement with single crystal hardness data reduced in this way (Evans & Goetze 1977).

(c) Stocker & Ashby used the simple Dorn law

$$\dot{\epsilon} = \dot{\epsilon}_0 \exp \left[\frac{-Q \{1 - (\sigma_1 - \sigma_3) / \sigma_p\}^2}{RT} \right] \quad (2)$$

for the portion above 8 kbar stress. In fact the Dorn law fits the data quite well down to 1–2 kbar differential stress, as can be seen in figure 4, in which differential stress is plotted against \sqrt{T} . A straight line on this plot represents a perfect fit to equation (2). The deviation at low stress corresponds to a transition to power law creep. Clearly, polycrystalline data do not at present constrain this power law region well, as most of them fall within the ‘Dorn range’ of rapidly varying stress exponent. The experimentally determined parameters for the Dorn range (figure 4 and equation (7)) differ markedly from those assumed by Stocker & Ashby.

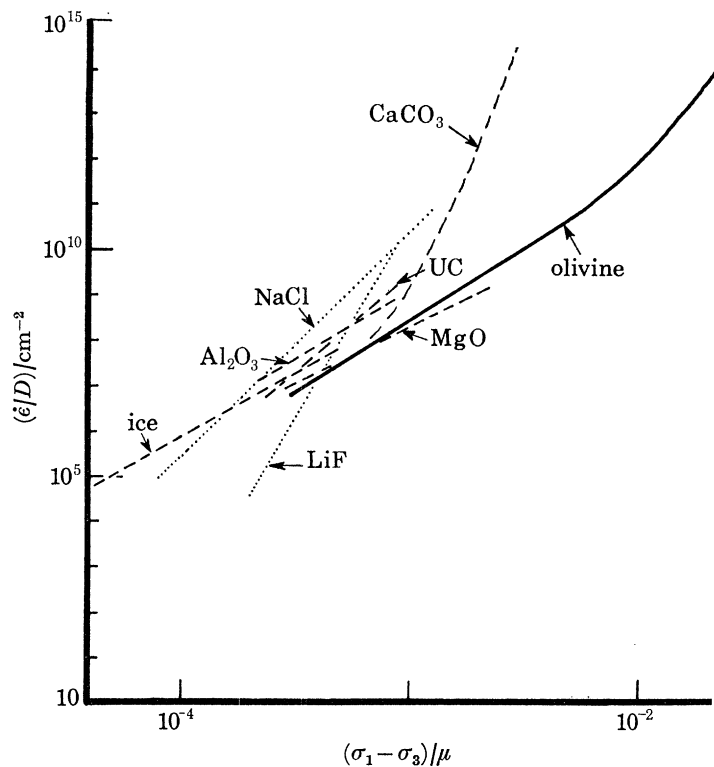


FIGURE 5. Data from figure 3 (solid line) are compared with corresponding data for a few materials showing power law creep (broken lines). Data are from Kirby & Raleigh (1973) except ice (Weertman 1972) and olivine (this study). When normalized in the manner shown (see text), materials exhibiting a cube dependence of strain rate on stress ($n = 3$) show similar absolute values of strain rate at low stresses. Olivine is no exception.

(d) Post's data show an obvious departure, greater than can be accounted for by experimental uncertainties, from the remaining data. The only reported difference between these results and the remaining data is the heat treatment (3 days at 950 °C in vacuum) to which the specimens were subjected before the deformation. Post's interpretation of this discrepancy is that trace quantities of hydrogen within the olivine lattice weaken the structure in a manner analogous to that shown to be true for variously orientated single crystals of quartz (hydrolytic weakening: Griggs 1967; Griggs & Blacic 1965; Heard & Carter 1968; Hobbs, McLaren & Paterson 1972) and that these heated specimens are drier (contain less hydrogen) than the remaining polycrystalline data. No measurements of hydrogen content have, however, been reported for any

of the polycrystalline specimens shown in figure 3. The fact that the hardness data were obtained on specimens of very low hydrogen content ($H/Si < 28/10^6$) argues against this interpretation. Post's data is also difficult to reconcile with creep data on single crystals of similarly low hydrogen content. Another possible explanation stems from the fact that the oxygen fugacity in the vacuum furnace was not controlled. It has recently become evident that the stability field of olivine with respect to oxygen fugacity is narrow at all temperatures (Nitzan 1974) and that heterogeneous precipitation of iron oxides onto all dislocations is rapid at 950 °C when the stability field is exceeded (Kohlstedt, Goetze & Durham 1976*b*; Kohlstedt & Vander Sande 1975). It has also been shown that such pinning of the dislocations increases the creep resistance of olivine (Carter & Ave' Lallemand 1970), and this could explain the unusual hardness of Post's specimens. Yet other explanations may be possible as well.

(*e*) Figure 5 shows a comparison of the data in figure 3 with a number of other materials displaying dislocation creep normalized to the form σ/μ against $\dot{\epsilon}/D$, where μ is an average elastic shear constant and D is the diffusivity controlling the climb process. A measurement of this D in olivine was made by Goetze & Kohlstedt (1973). A number of materials exhibiting dislocation creep show similar properties on this plot in the range $\sigma/\mu < 10^{-3}$ where climb could be a controlling factor (Kirby & Raleigh 1973). The two alkali halides have a higher stress exponent (n) and follow a somewhat different trend, although the absolute values are not too different from the remaining data with exponent near 3. Nabarro's pure climb model (1967) predicts strain rates about one to two orders of magnitude lower than the olivine curve and of slope $n = 3$. Our purpose here is simply to show that the absolute value of the strain rates for $\sigma/\mu < 10^{-3}$ are quite consistent with those measured on other $n \approx 3$ materials.

In summary, we can say that there is basically very good agreement among 'dry' polycrystalline data reported by a number of different laboratories using different apparatus and starting materials.

SINGLE CRYSTAL DATA

Olivine is one of comparatively few ceramic materials for which flow data is available for the primary, secondary and, at high temperatures, tertiary and quaternary slip systems. The primary data are the flow strengths of orientated single crystals of which three orientations are followed in figure 6 as a function of temperature and differential stress, again at a strain rate of 10^{-5} s^{-1} . The sources of single crystal data are given in the figure caption. The solid line indicates the trend of the data from figure 3 (equation 7). The orientation code $[110]_c$, indicates that σ_1 is orientated 45° from $[100]$ and $[010]$; $[101]_c$ indicates that σ_1 lies 45° from $[100]$ and $[001]$, etc. The flow curves of single crystals are similar to those of polycrystals in that work hardening becomes prominent at low temperatures, while at the highest temperatures crystals reach a steady-state creep rate in a strain of less than 1%, the transition occurring near 1000 °C (at $\dot{\epsilon} = 10^{-5} \text{ s}^{-1}$).

Slip systems

The slip systems by which these crystal orientations deform is given in the primary references and can be summarized as follows:

At intermediate temperatures a dramatic crossover occurs which is in excellent agreement with earlier reports of changes in the primary slip system with temperature (Raleigh 1965, 1968; Carter & Ave' Lallemand 1970). Near 1000 °C (at $\dot{\epsilon} = 10^{-5} \text{ s}^{-1}$) the slip systems $(001)[100]$ and $(010)[100]$ have very similar critical resolved shear stress, and a complex intermingling

of these systems occurs which macroscopically resembles pencil glide, $(0kl)[100]$ (Raleigh 1965, 1967, 1968; Carter & Ave' Lallemand 1970), but may result from extensive cross-slip on an atomic scale (Poirier 1975).

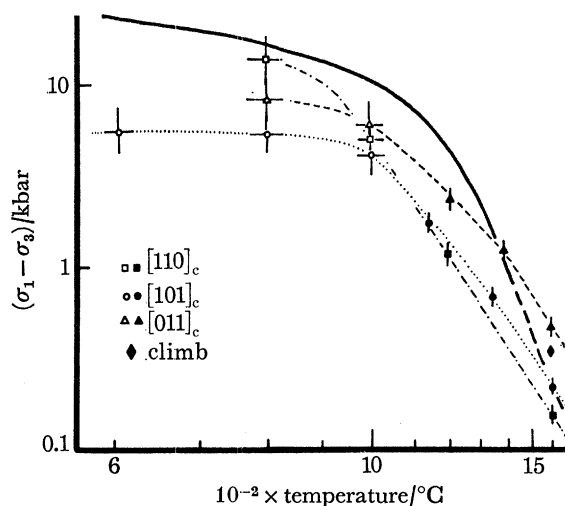


FIGURE 6. A comparison of the creep strength of three single crystal orientations and the trend of the polycrystalline data from figure 3 (solid curve). Temperature scale is linear in T^{-1} . Open circles are from Phakey *et al.* (1972), solid symbols from Durham & Goetze (1977).

TABLE 2

orientation	temperature	slip system(s)	Schmidt factor	reference
$[101]_c$	R.T. to 700 °C	$\{110\} [001]$	0.46	Evans & Goetze (1977)
$[101]_c$	800 °C	$\{110\} [001]$	0.46	Phakey <i>et al.</i> (1972)
$[101]_c$	890 °C	$\{110\} [001]$	0.46	Durham (1975)
$[101]_c$	1000 °C	$\{110\} [001]$	0.46	Phakey <i>et al.</i> (1972)
		+ (100) [001]	0.5	
		+ (?) [100]	?	
$[101]_c$	1600 °C	80% (001) [100] + 20% (100) [001]	0.5 0.5	Durham (1975)
$[011]_c$	800 °C	$\{110\} [001]$ + others?	0.21 ?	Phakey <i>et al.</i> (1972)
	1600 °C	(010) [001]	0.50	Durham (1975)
$[110]_c$	800–1000 °C	(010) [100]	0.50	Phakey <i>et al.</i> (1972)
	1600 °C	(010) [100]	0.50	Durham (1975)

Earlier data on the 'dominant slip systems' in polycrystalline specimens are reported in Raleigh (1965, 1967) and Carter & Ave' Lallemand (1970).

Climb

Six single crystal specimens deformed at 1600 °C (Durham & Goetze 1977a) did so with sufficiently uniform strain that a computer calculation could be used to isolate the proportion strain on the primary, secondary, etc., slip system. Of these the three $[101]_c$ orientation crystals showed that 10–15 % of the strain was accomplished by combined climb of $[100]$ and $[001]$ Burgers vector dislocations, presumably in the manner proposed by Nabarro (1967). The corresponding data are shown as a diamond in figure 6.

The Von Mises criterion

The Von Mises criterion states that five independent slip systems must be activated within polycrystalline grains if homogenous and pore-free deformation is to be achieved by slip alone (Von Mises 1928; Groves & Kelly 1963). In view of the fact that the strain is generally not homogeneous, there is general scepticism as to whether in fact all five systems are needed (Paterson & Weaver 1970). Paterson has convincingly shown through high-pressure deformation tests that two independent systems are not adequate for pore-free deformation, at least in the cases of MgO, NaCl, talc, pyrophyllite, graphite, and BN (Edmond & Paterson 1971, 1972).

The slip systems so far reported for olivine form three independent systems (see Phakey, Dollinger & Christie 1972). Shortening along any of the primary directions ([100], [010], [001]) requires a Burgers vector which does not lie along these directions. No such Burgers vector has so far been found. In the case of MgO, the pore-free polycrystalline flow law follows the flow law of crystals orientated for the hardest slip system required (Paterson & Weaver 1970). At an earlier stage of this study, the interpretation that the polycrystalline flow law approximated the upper envelope of the single crystal curves shown in figure 6 was considered. However, it now seems clear that the polycrystalline data lie at appreciably higher stress in the range 800–1300 °C (at $\dot{\epsilon} = 10^{-5} \text{ s}^{-1}$).

To our knowledge this is the first material with only three independent slip systems for which pore-free creep data has been reported. We are not aware of any theory for predicting the strength of materials whose individual slip systems do not form a complete set. The complex cross-over in individual slip system strengths shown near 1000 °C in figure 6 should provide an excellent test of such a theory once developed.

At the highest temperatures, climb provides the missing systems and the polycrystalline flow is therefore unlikely to fall outside the range 150–500 bar at 1600 °C ($\dot{\epsilon} = 10^{-5} \text{ s}^{-1}$).

DISLOCATION MECHANICS

The starting point for most dislocation models is the approximate relation

$$\dot{\epsilon} = \rho b \bar{v}, \quad (3)$$

where ρ is the mobile dislocation density, b the mean Burgers vector, and \bar{v} the mean dislocation velocity. We report here the progress made in understanding ρ and \bar{v} individually. Besides focusing attention on the processes actually controlling the creep mechanism, equation (3), if effective in predicting strain rates, has the potential to circumvent some of the problems inherent in extrapolating to lower strain rates. The dislocation mobilities can be followed to much lower temperatures and stresses than the corresponding strain rates. Actual dislocation velocities in the mantle are in the range 10^{-4} to $10^2 \mu\text{m/d}$ and with some patience an overlap may even be obtained with experimental mobility data. Actual dislocation densities can be inferred from those found in natural rocks. Such data can be combined through equation (3) to give an accurate picture of the flow law in a strain-rate range that cannot be sampled directly. In addition, a study of the dislocation microstructures has the potential for being inverted to permit an interpretation of the unknown deformation history of natural samples (Durham, Goetze & Blake 1977; Goetze 1975; Briegel & Goetze 1977).

Analysis of the dislocation structures has been made by transmission electron microscopy

(Phakey *et al.* 1972; Durham *et al.* 1977; Green & Radcliffe 1972*a, b, c*) and, where the dislocation density is low enough to view with the optical microscope ($< 10^8 \text{ cm}^{-2}$), by a low-temperature decoration technique (Kohlstedt *et al.* 1976*b*; Durham *et al.* 1977).

Dislocation density

The dislocation density is found to increase rapidly with strain to an equilibrium level, especially at low stress. An example of data from a single crystal sectioned at intervals of strain is shown in figure 7 (Durham *et al.* 1977). Plotting the equilibrium densities so achieved shows a strong correlation with the applied differential stress of the approximate form

$$\sigma_1 - \sigma_3 = \alpha \mu b \rho^{\frac{1}{2}} \quad (\text{Durham } et al. \text{ 1977}). \quad (4)$$

In figure 8, equilibrium dislocation density data for olivine are compared with corresponding data for quartz and calcite and a large class of materials displaying power law creep. The broken

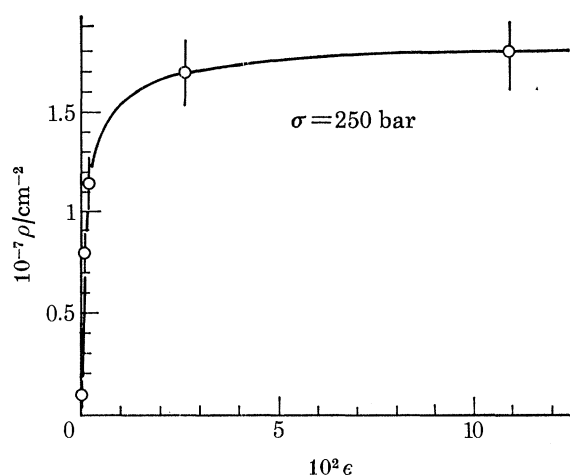


FIGURE 7. Dislocation density recorded in a single crystal of $[101]_c$ orientation from which sections were removed and decorated after strain increments of 0.12, 0.63, 2.9 and 11.1%.

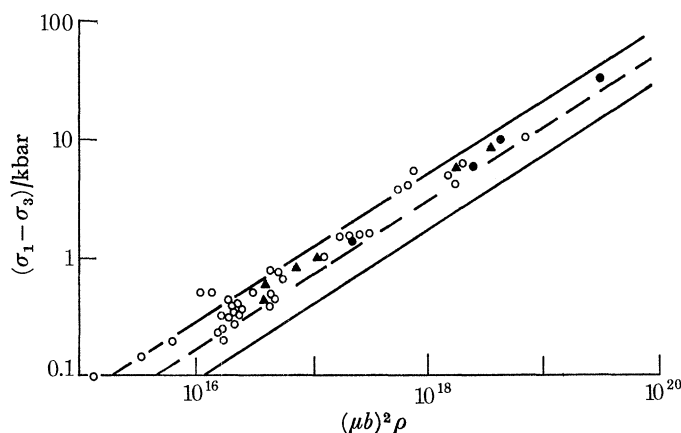


FIGURE 8. Steady-state dislocation densities recorded in olivine compared with quartz, calcite, and a summary of a large class of materials (pure metals, alloys, ionic solids) deforming by power law creep. The broken line is an average of the parameters in equation (4) from 33 such studies; the solid lines represent one standard deviation. In most studies, including olivine, a slope of greater than $\frac{1}{2}$ is indicated. The one shown is 0.62. This figure is from Durham *et al.* (1977): \circ , olivine; \bullet , quartz; \blacktriangle , calcite.

line is the mean correlation established from 33 studies on metals, alloys and ionic solids deforming by power law creep (Takeuchi & Argon 1976*b*) and the solid lines represent one standard deviation on either side. Clearly, olivine is no exception to this very general relation.

Glide velocity

One study has been done of the glide mobility on the (001) [100] and (010) [100] slip systems in the temperature range 1100–1600 °C (Durham *et al.* 1977). Unfortunately, the method did not yield data of high accuracy. However, the glide velocities so measured were very sluggish and of low stress sensitivity, as in the case of the diamond structure compounds (Alexander & Haasen 1968). When these measured glide velocities and the dislocation density from figure 8 are entered into equation (3), the predicted strain rates (small circles) fall close to the observed rates (large circles). Figure 9 shows this comparison for crystals of the orientation [101]_c gliding on the (001) [100] slip system. All data are again corrected to $\dot{\epsilon} = 10^{-5} \text{ s}^{-1}$. A similar result was obtained for the [110]_c orientation (Durham *et al.* 1977). We take this as an indication that,

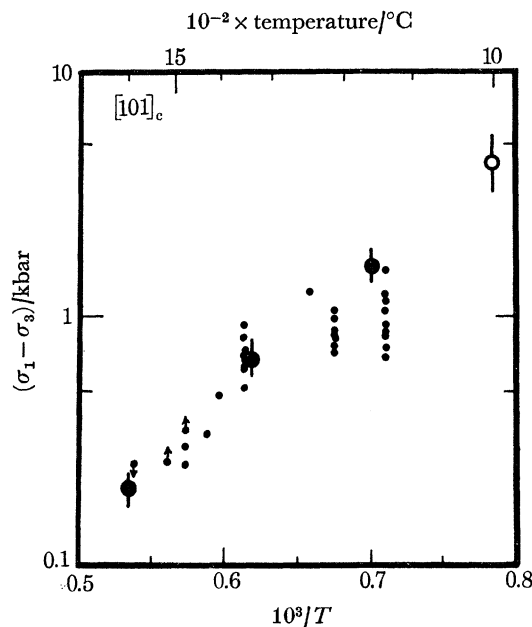


FIGURE 9. Comparison of observed strain rates (large circles) with strain rates predicted from equation (3), using experimentally determined dislocation densities and glide velocities, with $\dot{\epsilon}$ at 10^{-5} s^{-1} . Large open circle is from Phakey *et al.* (1972), solid large circles from Durham & Goetze (1977), and glide mobility data (small circles) from Durham *et al.* (1977).

for the range of variables tested, the observed density must be largely mobile and the glide velocity of the individual dislocations probably limits, or at least is close to limiting, the strain rate for single crystals of the orientations, temperatures and stresses sampled. There are also indications that the rate-insensitive glide stress on the (110) [001] system at low temperatures coincides with the appropriate shear stress at yield for the [101]_c orientation (Evans & Goetze 1977). It is therefore possible that the single crystal strengths are glide-controlled at low temperatures as well.

Whether the 'Dorn law' portion of the polycrystalline curve is also glide-controlled is a question we do not seek to answer here as we have no direct experimental evidence. The Dorn

law formulation was derived to represent the flow of materials exhibiting a high Peierls barrier in glide, and olivine appears to be such a material. However, the slip system of the glide mobility which is limiting the strain rate is not presently known (see discussion under Von Mises criterion). More work is needed to resolve this problem.

Climb velocity

Qualitative indications that climb is important above perhaps 1000 °C include (a) the 'picket fence' tilt boundaries frequently reported, in which the uniformity of the dislocation spacing could only be achieved through climb (Goetze & Kohlstedt 1973; Phakey *et al.* 1972; Green & Radcliffe 1972*b, c*) and (b) the heavily jogged glide loops observed as low stresses near 1600 °C (Durham *et al.* 1977). Quantitative estimates of climb mobility were obtained by Goetze & Kohlstedt (1973) and in the careful shape change measurements reported in Durham & Goetze (1977) and plotted in figure 6. These latter two cannot be directly compared, but it may be roughly said that glide and climb mobilities are approximately equal near 100 bar but that glide, having a higher stress sensitivity than climb (Durham *et al.* 1977), dominates at higher stress levels. Computer models of the dislocation mechanics for materials in which glide and climb mobilities are comparable (Takeuchi & Argon 1976*a*) show a number of striking similarities with the single crystal results obtained at 1600 °C and few hundred bars stress (Durham *et al.* 1977).

In summary, while figure 9 shows promise in separating the effect of dislocation density and dislocation mobility on the measured strain rates, there is ambiguity at low stresses whether glide or climb, or more likely some combination, limit the strain rates. The fact that both processes appear to have very similar rate sensitivities (see next section) indicates that a comparable mix will probably occur at much lower strain rates at the same stress level.

STRAIN RATE SENSITIVITY

It is of crucial importance for geological applications to be able to predict how figure 3 will change in going from a strain rate of 10^{-5} to geologically relevant strain rates in the range 10^{-15} to 10^{-10} s⁻¹. Qualitatively this curve will shift to lower temperatures. The extent to which it does so must at present be determined from strain rate sensitivity measurements within the experimentally accessible range of rates. These are assembled in figure 10.

The simple Dorn law,

$$\dot{\epsilon} = \dot{\epsilon}_0 \exp \left\{ -Q \left[1 - (\sigma_1 - \sigma_3) / \sigma_p \right]^2 RT \right\}, \quad (5)$$

has an apparent activation energy

$$Q_{app} = -R\Delta \ln \dot{\epsilon} / \Delta(1/T) = Q(1 - (\sigma_1 - \sigma_3) / \sigma_p)^2 \quad (6)$$

In view of the good fit of the hardness and polycrystalline data to this law (figure 4), the apparent activation energies for these data (1, 2, 3) were corrected by the factor $(1 - (\sigma_1 - \sigma_3) / \sigma_p)^{-2}$ to yield Q . This correction is comparatively minor below 10 kbar but substantial for the hardness point at 530 °C (1). We take the agreement between points 1, 2 and 3 as further evidence that the Dorn law is an appropriate form to use for the higher stress data. Points 6, 7 and 8 are apparent activation energies obtained from creep tests on single crystals, orientated for both single and multiple slip, deformed in the stress range in which glide and climb mobilities are comparable.

It is therefore uncertain which process controls the activation energy. Point 5 was obtained from the collapse rate of sessile dislocation loops and is presumed to represent the appropriate activation energy for the climb process alone. Point 4 was obtained from the temperature sensitivity of the annealing process in highly deformed olivine, a process which unquestionably involves a complex mix of glide and climb.

The single crystal data of Durham & Goetze (1977) contain data for the parameter

$$\left(\frac{\Delta \ln \sigma}{\Delta(1/T)}\right)_{\dot{\epsilon}} = - \left(\frac{\Delta \ln \dot{\epsilon}}{\Delta(1/T)}\right)_{\sigma} \cdot \left(\frac{\Delta \ln \sigma}{\Delta \ln \dot{\epsilon}}\right)_T = \frac{Q_{app}}{nR}$$

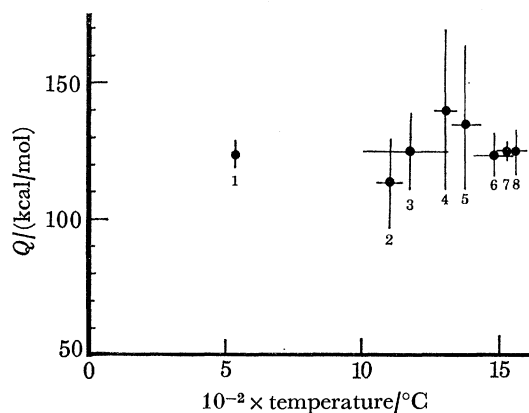


FIGURE 10. Activation energies measured for various processes. Horizontal bars show the temperature range over which the data were determined; vertical bars give standard deviation.

- (1) Hardness data (Evans & Goetze 1977);
- (2) polycrystalline flow (Kirby & Raleigh 1973);
- (3) polycrystalline flow (Carter 1976);
- (4) dislocation recovery (Goetze & Kohlstedt 1973);
- (5) climb, from collapse of sessile dislocation loops (Goetze & Kohlstedt 1973);
- (6) $[011]_0$ orientation single crystals (Durham & Goetze 1977);
- (7) single crystals orientated for multiple slip (Kohlstedt & Goetze 1974);
- (8) single crystals orientated for multiple slip (Durham & Goetze 1977).

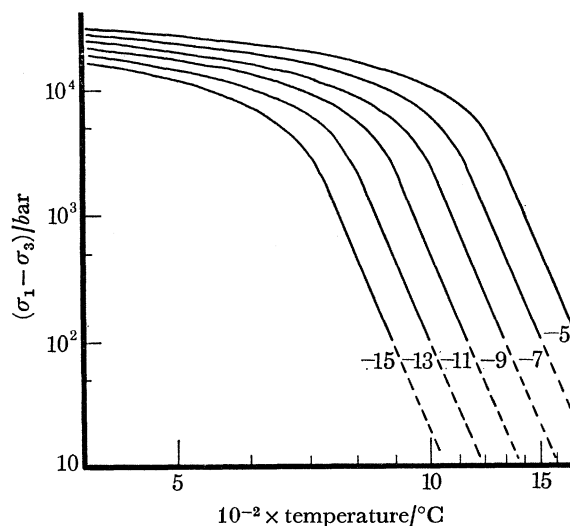


FIGURE 11. Extrapolation of the data in figure 3 to lower strain rates according to equation (7).

(n is the stress exponent in a local power law representation of the creep data), where Q_{app}/n drops at temperatures below about 1300 °C for several orientations. We do not feel that n is well enough determined for these specimens, however, to warrant any conclusion about the activation energy itself.

Apparently the processes likely to control the flow in the low stress region (0.1–1 kbar) is controlled by a similar, possibly identical, activation energy to that applicable to the Dorn region. We will not speculate here why this is so, but the practical consequence is that a simple extrapolation can be made using the Dorn law above 2 kbar and a power law below 2 kbar which will form continuous curves at all strain rates.

$$\begin{aligned} \sigma > 2 \text{ kbar: } \dot{\epsilon}/\text{s}^{-1} &= 5.7 \times 10^{11} \exp \left\{ -\frac{128 \text{ kcal/mol}}{RT} \left(1 - \frac{\sigma_1 - \sigma_3}{85000} \right)^2 \right\}; \\ \sigma < 2 \text{ kbar: } \dot{\epsilon} &= 70(\sigma_1 - \sigma_3)^3 \exp \{ -122(\text{kcal/mol})/RT \}. \end{aligned} \quad (7)$$

These curves are plotted in figure 11. A Q of 125 ± 10 kcal/mol appears to represent both processes; the values 122 and 128 kcal/mol were arbitrarily chosen to make a perfect match at all strain rates for numerical convenience. Stresses are given in bars in equations (7). In the stress and strain rate range of geologic interest the formal accuracy of equation (7) is better than ± 50 °C.

GRAIN-SIZE SENSITIVE CREEP

The boundary between dislocation creep and Coble creep is perhaps the least well determined in the deformation map shown in figure 2, as there are very meagre data on which to base the necessary systematics. Bouillier & Gueguen (1975) presented convincing evidence that some form of grain-size sensitive creep has occurred in a number of highly mylonitized natural specimens. Schmid (1976) and Schmid, Boland & Paterson (1977) have found a grain-size sensitive flow field in a recent laboratory deformation study on very fine-grained limestones, but so far there has been no comparable study, to my knowledge, on fine-grained olivine aggregates. Recently two indirect pieces of evidence have come to light that constrain the boundary between dislocation creep and a grain-size sensitive creep field, and in view of the importance of this subject these will now be briefly reviewed.

It has long been known that creep experiments on olivine aggregates in the differential stress range 1–10 kbar occasionally show ‘ductile faulting’ (Blacic 1972; Post 1973), a process in which the development of a fine-grained shear zone, resembling a fault but apparently devoid of porosity, is accompanied by a marked drop in stress, presumably indicating a grain-size sensitive enhancement of the flow within the shear zone. Twiss (1976) has extracted from Post’s thesis four (‘dry’) specimens for which the relevant variables can be estimated. The four points so obtained are, however, sufficiently close together in stress, temperature, grain size, and strain rate that the dependence of none of these variables can be extracted from the data alone.

A second source comes from hot-pressing studies on samples of olivine powders ranging in grain size from 5–2000 μm (Schwenn & Goetze 1977; Schwenn 1976). Hot-pressing characteristics were found to be controlled by power law creep at large grain sizes and by a very grain-size sensitive flow law at small grain sizes for which strain rate varied as grain size raised to the power -2 to -4.5 and stress raised to the power 1.1–1.9. Using the relations between hot-pressing and creep characteristics (Wilkinson & Ashby 1975, 1976; Coble 1970), the creep law for the corresponding dense material was derived. It predicts the four data points extracted

by Twiss within a factor of 3 in strain rate. This flow law is given below, together with the corresponding flow law predicted by Stocker & Ashby on the basis of systematics.

Schwenn & Goetze:

$$\dot{\epsilon} = (3-10) \times 10^4 (\sigma_1 - \sigma_3) s_g^{-3} \exp \{ -85(\text{kcal/mol})/RT \}. \quad (8a)$$

Stocker & Ashby:

$$\dot{\epsilon} = 0.5 (\sigma_1 - \sigma_3) T^{-1} s_g^{-3} \exp \{ -103(\text{kcal/mol})/RT \}. \quad (8b)$$

(Parameters are for stress in bars and grain size (s_g) in centimetres.)

As the creep rate in these laws is presumably controlled by the grain boundary diffusivity, it is not yet clear to what extent impurities along the grain boundaries will cause a wide scatter among different determinations of the flow parameters. However, the several groups now working on this problem should provide some answer to this question within a year or two.

TABLE 3. EXPERIMENTALLY DETERMINED CONSTANTS FOR EQUATION (9)

reference	A	b
Post (1973)	40	-0.67
Kohlstedt <i>et al.</i> (1976a)	76	-0.63
Carter & Mercier (1976)	49	-0.71

Constants are for stress in bars and grain size in centimetres

One important question to investigate is whether any of the experimental data now in hand in fact fall within this Coble creep field. Taking the reported starting grain sizes as representative of the run, we find that only the data for creep of Mt Albert peridotite reported by Goetze & Brace (1972) fall in this category. However, many of the data between 1 and 10 kbar are obtained from specimens which partially recrystallized during the deformation experiment.

A number of authors have investigated this dynamic recrystallization process in olivine (Ave' Lallemand & Carter 1970; Kirby & Raleigh 1973; Post 1973; Carter & Mercier 1976) and the results may be briefly summarized as follows. With increasing strain a new generation of grains appears, principally along the grain boundaries of the starting material, and gradually replaces the starting grain structure. The new grain size so formed appears to correlate with stress according to the relation

$$\sigma_1 - \sigma_3 = Ad^b, \quad (9)$$

where table 3 gives the parameters A and b according to three different studies. Post's are the only parameters for which flow data and grain size are reported on the same specimens. The parameters given by Kohlstedt *et al.* (1976a) are based primarily on naturally deformed specimens. All three make very similar predictions in the grain size range in which the data overlap. Similar results have been reported for α -iron (Glover & Sellars 1973) and Ni-Fe alloys (Luton & Sellars 1969).

Combining Post's parameters in equation (9) with equation (8a) provides a prediction for the strain rate of a fully recrystallized specimen. It is an empirically established Coble creep law:

$$\dot{\epsilon} = 3.6 \times 10^{11} (\sigma_1 - \sigma_3)^{5.47} \exp (-85000/RT). \quad (10)$$

We use Post's parameters because we will shortly make a comparison with creep data obtained on the same specimens. In figure 12 we compare this flow law with the law appropriate to coarse grain sizes taken from figures 3 and 11, again for a constant strain rate of 10^{-5} s^{-1} . The clear

indication is that specimens which are fully recrystallized will be softer than the coarser-grained starting material over a range of differential stress from approximately 1 to 15 kbar (at $\dot{\epsilon} = 10^{-5} \text{ s}^{-1}$). It is apparent in retrospect, therefore, that the interpretation of data in this range is potentially treacherous since specimens might show any strength between that predicted by the Coble law and that predicted by the dislocation creep law of figure 11, depending on the degree of recrystallization, a fact which was not appreciated at the time the experiments were done. The reasons for a variety of complexities in the original records, such as ductile faulting,

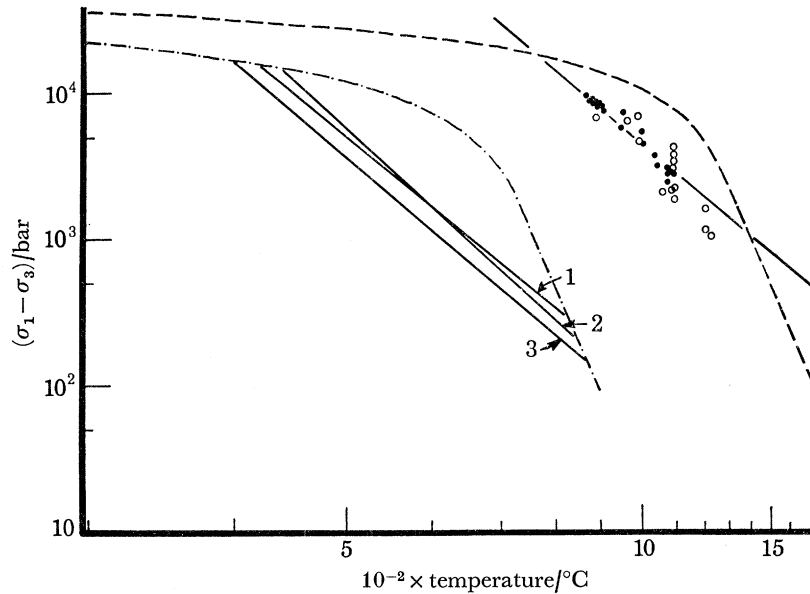


FIGURE 12. On the right: a comparison of the data from figure 3 (broken line) with the strengths predicted from the experimentally determined Coble creep parameter (equation (8a)) and grain sizes (equation (9)) for $\dot{\epsilon} = 10^{-5} \text{ s}^{-1}$ (solid line, Post 1973). The 'wet' data of Post (1972) (●) and Carter & Ave' Lallemand (1970) (○) appear to coincide with this line. On the left: the corresponding lines extrapolated to a strain rate of 10^{-15} s^{-1} : 1, Kohlstedt *et al.* (1976a); 2, Murrell & Chakravarty (1973); 3, Post (1973).

are now readily understood. It is also instructive to plot the 'wet' olivine data which are shown as circles in figure 12 (data for $\dot{\epsilon} = 10^{-6}$ to 10^{-4} s^{-1} are corrected to 10^{-5} as before). The tendency for these data to fall along the Coble creep line is marked especially in the case of Post's wet data which show low scatter and for which the grain size parameters leading to the Coble line shown were determined. Carter & Ave' Lallemand's (1970) data can be interpreted as showing a wider scatter about the same line. This suggests an interpretation of the 'wet' data as simply more completely recrystallized than the 'dry' data, rather than a hydrolytic weakening of the crystals themselves, as suggested by Post (1973), Carter & Ave' Lallemand (1970), Blacic (1972), and others. This is also consistent with our own inability to find any evidence of hydrolytic weakening in olivine single crystals in spite of repeated attempts.

The effect of moisture is, in this interpretation, only indirectly related to the strength through the degree of recrystallization. It appears unlikely at present that water affects the Coble creep process directly since the hot-pressing data were obtained under both hydrous and non-hydrous atmospheres at 1 bar total pressure and Twiss's data were extracted from ductile faulting which occurred in Post's 'dry' experiments. In fact, Post systematically rejected 'dry' runs which showed a falling stress, believing them not to be 'completely dry'. Moisture therefore does not

appear to be a prerequisite for observing the Coble creep process given by equation (10). It is very likely that new data will modify this simple picture, but the recognition that the 'wet' data fall within the Coble creep field could help unravel this longstanding problem.

As a last bit of speculation we might consider what implications the empirically determined Coble creep law has for deformation within the mantle at geological strain rates. In figure 12 we have plotted the same comparison between dislocation and Coble creep strengths extrapolated to $\dot{\epsilon} = 10^{-15} \text{ s}^{-1}$. All three sets of parameters shown in table 3 have been inserted in equations (8a) and (9) to give appropriate versions of equation (10). These have all been plotted in figure 12 to give an illustration of the range of flow stress predicted by table 3. The parameters given by Kohlstedt *et al.* (1976a) are based primarily on natural specimens deformed at geologic strain rates and give some justification for using the experimental grain size/stress relation under geological conditions. The marked increase in the stress range dominated by the Coble process at $\dot{\epsilon} = 10^{-15} \text{ s}^{-1}$ over that at $\dot{\epsilon} = 10^{-5} \text{ s}^{-1}$ results from the lower apparent activation energy of the Coble process.

At the highest stresses observed in natural specimens (1–3 kbar) the dominant creep mechanism is almost surely Coble creep, *if* recrystallization is permitted to go to completion. The introduction of grain size as a variable in the flow law creates an apparent strain or time dependence of lithospheric strength not present with the dislocation mechanism alone. After static annealing or crystallization from the melt, for example, a rock may have a comparatively large grain size ($> 500 \mu\text{m}$) and be initially quite strong. There will be a stress level (such as 1 kbar at 600°C , for example, in figures 11 and 12) at which this coarse material will strain at a geologically negligible rate and therefore never recrystallize. However, if a fine grain size is introduced through a fracture, or if the stress is raised to the point where the strain rate becomes appreciable and recrystallization begins, then this region will strain-soften rapidly. Strain-softening is the principal requirement for concentrating strain into shear zones which could form the downward extension of the brittle faulting found at shallow depths. A fault, once begun, can extend itself downwards by the stress concentrations near its leading edge to result in a band of fine recrystallized material – a permanent zone of weakness through the lithosphere until static annealing returns it to a coarse grain size. Such a material can show a surprisingly complex repertoire of mechanical behaviour, much of which has its analogue in geological field evidence. Understanding these lithospheric deformations remains a promising but undeveloped field.

According to figure 12, the region below the intersection near $\sigma_1 - \sigma_3 = 200 \text{ bar}$ should be dominated by power law creep. This region in stress corresponds to the asthenosphere in the Earth. One may confirm this conclusion by substituting the grain size observed in rocks from the upper mantle (1–10 mm) in equation (8) rather than by using the empirical grain size/stress correlation, equation (9). Twiss (1976) predicts that the Coble process will dominate to stresses as low as 20 bar. This discrepancy between our conclusions does not result from different predictions about the Coble process, however, but from the very 'hard' dislocation creep formula used by Twiss which, although apparently based on Post's 'dry' measurements (see figure 3), is more creep-resistant than any experimental data of which this author is aware. Nevertheless, an improved value for this important boundary between the two mechanisms awaits better data.

CONCLUSIONS

(1) There is fairly good agreement and understanding of the dislocation creep field, at least within the range of strain rates which can be explored in the laboratory.

(2) Some experimental data now exist on a grain-size sensitive flow law, phenomenologically resembling the Coble creep mechanism. In the Earth this mechanism is expected to dominate the deformation of olivine at the high stresses (0.3–3 kbar) characteristic of the lithosphere if dynamic recrystallization to small grain sizes occurs. It appears unlikely that it will dominate in the differential stress range 10–100 bar characteristic of the asthenosphere.

(3) The previously designated 'wet' data probably correspond to this grain-size sensitive flow law.

Support from National Science Foundation grant no. DES72-01676 A03 is gratefully acknowledged.

REFERENCES (Goetze)

- Alexander, H. & Haasen, P. 1968 Dislocations and plastic flow in the diamond structure. *Solid State Phys.* **22**, 27–158.
- Auten, T. A. & Radcliffe, S. V. 1976 Deformation of polycrystalline MgO at high hydrostatic pressure. *J. Am. ceram. Soc.* **59**, 249–253.
- Ave' Lallemand, H. G. & Carter, N. L. 1970 Syntectonic recrystallization of olivine and modes of flow in the upper mantle. *Bull. geol. Soc. Am.* **81**, 2203–2220.
- Blacic, J. D. 1972 Effect of water on the experimental deformation of olivine. In *Flow and fracture of rocks* (eds H. C. Heard, I. Y. Borg, N. L. Carter & C. B. Raleigh), pp. 109–115. Am. geophys. Union Monograph no. 16.
- Bouillier, A. M. & Gueguen, Y. 1975 Origin of some mylonites by superplastic flow. *Contrib. Mineral. Petrol.* **50**, 93–104.
- Briegel, U. & Goetze, C. 1977 Estimate of stress in Lochseiten limestone with dislocation densities. *Tectonophysics* (In the press.)
- Carter, N. L. & Ave' Lallemand, H. G. 1970 High temperature flow of dunite and peridotite. *Bull. geol. Soc. Am.* **81**, 2181–2202.
- Carter, N. L. 1976 Steady-state flow of rocks. *Rev. Geophys. & Space Phys.* **14**, 301–360.
- Carter, N. L. & Mercier, J.-C. C. 1976 Stress dependence of olivine neoblast grain sizes. *Trans. Am. geophys. Un., Eos* **57**, 322.
- Coble, R. L. 1970 Diffusional models for hot-pressing with surface energy and pressure effects as driving forces. *J. appl. Phys.* **41**, 4798–4807.
- Deer, W. A., Howie, R. A. & Zussman, J. 1964 *Rock-forming minerals*, vol. 1, pp. 12–13. London: Longmans Green.
- Durham, W. B. 1975 Plastic flow of single-crystal olivine. Ph.D. thesis, Massachusetts Institute of Technology, Cambridge, Massachusetts.
- Durham, W. B. & Goetze, C. 1977a Plastic flow of oriented single crystals of olivine. I. Mechanical data. *J. geophys. Res.* (In the press.)
- Durham, W. B. & Goetze, C. 1977b A comparison of the creep properties of pure forsterite and iron-bearing olivine. *Tectonophysics* (In the press.)
- Durham, W. B., Goetze, C. & Blake, B. 1977 Plastic flow of oriented single crystals of olivine. II. Observations and interpretations of the dislocation structures. *J. geophys. Res.* (In the press.)
- Eaton, S. F. 1968 The high temperature creep of dunite. Ph.D. thesis, Princeton University.
- Edmond, J. M. & Paterson, M. S. 1971 Strength of solid pressure media and implications for high pressure apparatus. *Contrib. Mineral. Petrol.* **30**, 141–160.
- Edmond, J. M. & Paterson, M. S. 1972 Volume changes during deformation of rocks at high pressures. *Int. J. rock Mech. & min. Sci.* **9**, 161–182.
- Evans, B. & Goetze, C. 1977 Manuscript in preparation.
- Glover, G. & Sellars, C. M. 1973 Recovery and recrystallization during high temperature deformation of α -iron. *Metall. Trans.* **4**, 765–775.
- Goetze, C. & Brace, W. F. 1972 Laboratory observations of high-temperature rheology of rocks. *Tectonophysics* **12**, 583–600.

- Goetze, C. 1971 High temperature rheology of Westerly granite. *J. geophys. Res.* **76**, 1223–1230.
- Goetze, C. 1975 Sheared lherzolites: from the point of view of rock mechanics. *Geology* **3**, 172–173.
- Goetze, C. & Kohlstedt, D. L. 1973 Laboratory study of dislocation climb and diffusion in olivine. *J. geophys. Res.* **78**, 5961–5971.
- Green, H. W. & Radcliffe, S. V. 1972*a* The nature of deformation lamellae in silicates. *Bull. geol. Soc. Am.* **83**, 847–852.
- Green, H. W. & Radcliffe, S. V. 1972*b* Dislocation mechanisms in olivine and flow in the upper mantle. *Earth & planet. Sci. Lett.* **15**, 239–247.
- Green, H. W. & Radcliffe, S. V. 1972*c* Deformation processes in the upper mantle. In *Flow and fracture of rocks* (eds H. C. Heard, I. Y. Borg, N. L. Carter & C. B. Raleigh), pp. 139–157. Am. geophys. Un. Monograph, no. 16.
- Griggs, D. T. & Blacic, J. D. 1965 Quartz: anomalous weakness of synthetic crystals. *Science N.Y.* **147**, 292–295.
- Griggs, D. T. 1967 Hydrolytic weakening of quartz and other silicates. *Geophys. J. R. astron. Soc.* **14**, 19–31.
- Groves, G. W. & Kelly, A. 1963 Independent slip systems in crystals. *Phil. Mag.* **8**, 877–887.
- Handin, J. 1966 Strength and ductility, in *Handbook of physical constants* (ed. S. P. Clark, Jr). Geol. Soc. Am. Memoir, no. 97.
- Heard, H. C. & Carter, N. L. 1968 Experimentally induced ‘natural’ intragranular flow in quartz and quartzite. *Am. J. Sci.* **266**, 1–41.
- Hobbs, B. E., McLaren, A. C. & Paterson, M. S. 1972 Plasticity of single crystals of synthetic quartz. In *Flow and fracture of rocks* (eds H. C. Heard, I. Y. Borg, N. L. Carter & C. B. Raleigh), pp. 29–53. Am. geophys. Un. Monograph no. 16.
- Johnson, K. L. 1970 The correlation of indentation experiments. *J. Mech. Phys. Solids* **18**, 115–126.
- Kirby, S. H. & Raleigh, C. B. 1973 Mechanisms of high-temperature, solid state flow in minerals and ceramics and their bearing on creep behaviour of the mantle. *Tectonophysics* **19**, 165–194.
- Kohlstedt, D. L. & Goetze, C. 1974 Low-stress high-temperature creep in olivine single crystals. *J. geophys. Res.* **79**, 2045–2051.
- Kohlstedt, D. L., Goetze, C. & Durham, W. B. 1976*a* Experimental deformation of single crystal olivine with application to flow in the mantle. In *The physics and chemistry of minerals and rocks* (ed. S. K. Runcorn), pp. 35–49. London: John Wiley.
- Kohlstedt, D. L., Goetze, C., Durham, W. B. & Vander Sande, J. B. 1976*b* A new technique for decorating dislocations in olivine. *Science, N.Y.* **191**, 1045–1046.
- Kohlstedt, D. L. & Vander Sande, J. B. 1975 Heterogeneous precipitation on dislocations in olivine. *Contrib. Mineral. Petrol.* **53**, 13–25.
- Langdon, T. G., Cropper, D. R. & Pask, J. A. 1971 Creep mechanisms in ceramic materials at elevated temperatures. In *Ceramics in severe environments*, vol. 5, pp. 297–315. Materials Science Research, New York: Plenum Press.
- Luton, M. J. & Sellars, C. M. 1969 Dynamic recrystallization in Ni and Ni–Fe alloys during high temperature deformation. *Acta metall.* **17**, 1033–1043.
- Misra, A. K. & Murrell, S. A. F. 1965 An experimental study of the effect of temperature and stress on the creep of rocks. *Geophys. J. R. astron. Soc.* **9**, 509–535.
- Murrell, S. A. F. & Chakravarty, S. 1973 Some new rheological experiments on igneous rocks at temperatures up to 1120 °C. *Geophys. J. R. astron. Soc.* **34**, 211–250.
- Nabarro, F. R. N. 1967 Steady-state diffusional creep. *Phil. Mag.* **16**, 231–239.
- Nitzan, U. 1974 Oxidation and reduction of olivine. *J. geophys. Res.* **79**, 706–711.
- Paterson, M. S. & Edmond, J. M. 1972 Deformation of graphite at high pressures. *Carbon* **10**, 29–34.
- Paterson, M. S. & Weaver, C. W. 1970 Deformation of polycrystalline MgO under pressure. *J. Am. ceram. Soc.* **53**, 463–471.
- Phakey, P., Dollinger, G. & Christie, J. 1972 Transmission electron microscopy of experimentally deformed olivine crystals. In *Flow and fracture of rocks* (eds H. C. Heard, I. Y. Borg, N. L. Carter & C. B. Raleigh), pp. 117–138. Am. geophys. Un. Monograph, no. 16.
- Poirier, J. P. 1975 On the slip systems of olivine. *J. geophys. Res.* **80**, 4059–4061.
- Post, R. L., Jr 1973 High temperature creep of Mt Burnet dunite. Ph.D. thesis (geophysics), University of California at Los Angeles.
- Raleigh, C. B. 1965 Glide mechanisms in experimentally deformed minerals. *Science, N.Y.* **150**, 739–741.
- Raleigh, C. B. 1967 Plastic deformation of upper mantle silicate minerals. *Geophys. J. R. astron. Soc.* **14**, 45–49.
- Raleigh, C. B. 1968 Mechanisms of plastic deformation of olivine. *J. geophys. Res.* **73**, 5391–5407.
- Raleigh, C. B. & Kirby, S. H. 1970 Creep in the upper mantle. *Mineral. Soc. Am. Spec. Paper*, **3**, 113–121.
- Schmid, S. M. 1976 Rheological evidence for changes in the deformation mechanism of Solenhofen limestone towards low stresses. *Tectonophysics* **31**, T21–T28.
- Schmid, S. M., Boland, J. N. & Paterson, M. S. 1977 Superplastic flow in fine-grained limestone. *Tectonophysics* (In the press.)
- Stocker, R. L., & Ashby, M. F. 1973 On the rheology of the upper mantle. *Rev. Geophys.* **11**, 391–497.

- Schwenn, M. B. 1976 The creep of olivine during hot-pressing. S.M. thesis in geophysics, Massachusetts Institute of Technology, Cambridge, Massachusetts.
- Schwenn, M. B. & Goetze, C. 1977 Creep of olivine during hot-pressing. *Tectonophysics* (In the press.)
- Takeuchi, S. & Argon, A. S. 1976*a* Steady-state creep of alloys due to viscous motion of dislocations. *Acta metall.* **24**, 883–890.
- Takeuchi, S. & Argon, A. S. 1976*b* Steady-state andrade creep of single-phase crystals at high temperature. *J. mater. Sci.* **11**, 1542–1566.
- Twiss, R. S. 1976 Structural superplastic creep and linear viscosity in the earth's mantle. *Earth & planet. Sci. Lett.* **33**, 79–86.
- Von Mises, W. 1928 Mechanik der plastischen Formänderung von Kristallen. *Z. angew. Math. Mech.* **8**, 161.
- Weertman, J. 1972 Creep of ice. In *The physics and chemistry of ice* (eds E. Whalley, S. J. Jones & L. W. Gold), pp. 320–337. Ottawa: Royal Society of Canada.
- Weertman, J. 1970 The creep strength of the earth's mantle. *Rev. Geophys.* **8**, 145–168.
- Wilkinson, D. S. & Ashby, M. F. 1975 Pressure sintering by power law creep. *Acta metall.* **23**, 1277–1285.
- Wilkinson, D. S. & Ashby, M. F. 1976 The development of pressure sintering maps. *Proc. 4th Int. Cong. on Sintering and Related Phenomena*, May 26–28, 1975. (In the press.)

Discussion

J. P. POIRIER (*Saclay, France*). Following Professor Goetze's interesting considerations on the glide and climb of edge dislocations, I should like to make a few remarks on the mobility of screw dislocations in olivine:

- (1) Numerous long and straight [100] screw dislocations are very often observed in olivine crystals experimentally or naturally deformed at high temperature. These dislocations obviously move with great difficulty.
- (2) Similar straight screw dislocations are known to be present in body-centred cubic metals at low temperatures. This has been explained by the fact that dislocations are split on several planes. We have recently shown that such a multiple splitting is also possible for [100] screw dislocations in olivine on (010) and (001) planes.
- (3) Thus, the mobility of [100] screws in glide and/or cross-slip is probably controlled by the pinching of one of the stacking fault ribbons.
- (4) If the mobility of slow moving screws contributes to the control of high temperature creep of olivine and if hydrostatic pressure favours the pinching of the stacking fault ribbons as is the case with sodium chloride, then the effective activation volume could be much smaller than the activation volume for diffusion controlled climb.